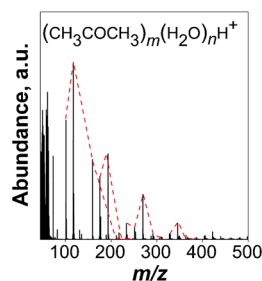


RESEARCH ARTICLE

Insights on Clusters Formation Mechanism by Time of Flight Mass Spectrometry. 2. The Case of Acetone–Water Clusters

B. Apicella,¹ X. Li,^{1,2} M. Passaro,^{1,3} C. Russo¹¹Istituto di Ricerche sulla Combustione, IRC–CNR, P.le Tecchio 80, 80125, Napoli, Italy²Key Laboratory of Power Machinery and Engineering, Ministry of Education, Shanghai Jiao Tong University, Shanghai, 200240, China³Chemical Engineering, Materials and Industrial Production Department, University of Naples “Federico II”, P.le Tecchio 80, 80125, Napoli, Italy

Abstract. This paper is the second of a series dealing with clusters formation mechanism. In part 1, water clusters with the addition of an electrophilic molecule such as ethanol were studied by Time Of Flight Mass Spectrometry (TOFMS). Mass distributions of molecular clusters of ethanol, water and ethanol–water mixed clusters, were obtained by means of two different ionization methods: Electron Ionization (EI) and picosecond laser Photo–ionization (PI) at a wavelength of 355 nm. In part 2, the same experimental approach was employed to obtain mass spectra of clusters generated by acetone–water binary mixtures with a different composition. Strong dependence of the mass spectra of clusters with EI and PI on the acetone–water mixing ratio was observed. It was shown that the spectral pattern changes gradually

and water-rich cluster signals become fainter while acetone-rich cluster signals become more intensive with increasing acetone concentrations from 0.3% to 40%. Owing to the hydrogen bond acceptor character of acetone, its self-association is discouraged with respect to ethanol. The autocorrelation function (AF) was used to analyze the variation of the water clusters composition with the increase of the acetone concentration in terms of fundamental periodicities. However, although acetone and ethanol present a very different hydrogen-bonding ability, similarly to ethanol–water system, in acetone–water system the formation of water-rich clusters and subsequent metastable fragmentation are the dominant process that determine the clusters distribution, irrespective of the ionization process, while the ionization process significantly affects the acetone-rich clusters distribution.

Keywords: Acetone–water clusters, Reflectron time-of-flight mass spectrometry, Short-pulse laser, Photo-ionization

Received: 19 May 2016/Revised: 20 July 2016/Accepted: 22 July 2016/Published Online: 29 August 2016

Introduction

Many papers were published on water clusters, mainly aiming at the possibility of using them as a vehicle to study molecular properties of water systematically [1–8]. However, not all is known about the different size water clusters formation and ionization.

In this work, water clusters were produced in a supersonic expansion and studied by a Time Of Flight Mass

Spectrometer (TOFMS) using an electron beam and a laser beam as ionization sources. In order to deep the knowledge of cluster formation, two kinds of additives were added to water clusters: ethanol and acetone. Both additives have higher proton affinities with respect to water (acetone more than ethanol) and thus changing the cluster network. Indeed, when a solvent molecule is replaced by another molecule with larger proton affinity, the strength of all other hydrogen bonds decreases, on the basis of the concept of “anticooperativity” through successive substitutions in a mixed solvation system introduced in [8, 9]. However, both ethanol and acetone present a very different hydrogen-bonding ability: ethanol molecules have both H-bond acceptor and donor sites, whereas acetone

Electronic supplementary material The online version of this article (doi:10.1007/s13361-016-1464-3) contains supplementary material, which is available to authorized users.

Correspondence to: B. Apicella; e-mail: apicella@irc.cnr.it

molecules have only acceptor sites (two lone pairs). This difference enables different water-water/ water-additive/ additive-additive interactions whose study will make it possible to deepen the mechanisms of cluster formation.

The results obtained with ethanol are reported in a previous paper [8], which constitutes part 1 of a 2 parts series. The results on acetone and the comparison with ethanol-water mixed clusters are reported in this paper, which is part 2.

Moreover, acetone-water mixtures constitute interesting systems to be investigated and have been the subject of many studies also because the acetyl radical is important in atmospheric reactions and as it contains two equivalent C-C bonds. A study on acetone-water clusters showed that the lifetime of the excited acetone moiety increases substantially from less than 100 fs in the case of an acetone molecule to a few picoseconds for both pure acetone and mixed acetone-water clusters [10]. This indicates that the presence of water-acetone clusters will affect the lifetime of acetone in the atmosphere at higher altitudes and lower temperatures. Therefore, more attention should be paid on water-acetone binary mixtures.

In the past decade, great attention was put on the non-ideal characteristic of binary mixtures of organic solvents, such as methanol, ethanol, acetonitrile, etc., with water [11–15]. These studies on the organic solvent-water clusters indicate that the deviations from ideality are due to intermolecular interactions in the mixture system. The incomplete mixing was suggested for methanol-water binary mixtures on the basis of neutron diffraction experiments by Dixit et al. [16]. They noted that the local structure of water in a concentrated methanol-water solution is surprisingly close to its counterpart in pure water. Comparing the cluster structures of water-methanol, -ethanol, -1-propanol, -1-butanol, -1-pentanol, Wakisaka et al. [12] suggested that microscopic phase separation occurs in all of alcohol-water binary mixtures and they found that if the size of the hydrophobic group of alcohols was increased, methyl→ethyl→butyl, the alcohol-alcohol interactions occurred easily. For example, the water-butanol system with a molar ratio of $\text{H}_2\text{O}:\text{C}_4\text{H}_9\text{OH} = 300:1$ showed the same type of mass spectrum as the water-methanol system with $\text{H}_2\text{O}:\text{CH}_3\text{OH} = 100:1$. It means that alcohol-alcohol interactions occur more easily for alcohols with a larger hydrophobic group [12]. Wakisaka et al. [13] studied isolated clusters from water-methanol and water-acetonitrile binary mixtures too and suggested that the interaction of water with methanol is quite different from the one with acetonitrile. Methanol molecules have a substitutional interaction with water clusters, while acetonitrile molecules have an additional interaction with water clusters. This is why methanol can both donate and accept hydrogen bonds, whereas acetonitrile can only accept hydrogen bonds. Binary mixtures of acetone-water, acetonitrile-water, and methanol-water mixtures were investigated over the whole composition range by Venables et al. [3]. They reported that infrared spectra of acetone and acetonitrile mixtures with water are similar, exhibiting a slight blue-shift as the co-solvent is added to water, followed by a large red-shift at a high co-

solvent concentration. On the contrary, the spectra of methanol-water mixtures are blue-shifted over their whole composition, and that indicated a strengthening in structure in the methanol-water binary mixture and a weakening in the interaction between molecules in acetone-water mixture and acetonitrile-water mixture. The hydrogen bonding in the mixtures was examined in greater details than previously. The tetrahedral structure of water is lost when the co-solvent concentration increases, but three and two hydrogen bonded water molecules remain over an extensive range of compositions. Water molecules have a tendency to aggregate in all mixtures, but in acetone and acetonitrile mixtures this tendency was especially marked. The detailed evaluation of the static connectivity of water molecules is only a first step to understand the water hydrogen bonding network. Evaluating how the hydrogen bonding network changes in time should make it possible to broaden our knowledge about cooperative motions in water. Efforts towards this end are currently being pursued. These results indicate that the non-ideal characteristics of mixing of organic solvents with water are general. But, this mixing is very complex because it is affected by the molecular structure of the solvent, mixing ratios, temperature, etc.

Photo-Ionization (PI) [including Single-Photon Ionization (SPI) and Multi-Photon Ionization (MPI)] in combination with Time Of Flight Mass Spectrometry (TOFMS) was demonstrated to be a powerful technique to study the non-ideal characteristics of organic solvent mixtures based on the observation and analysis of their clusters [10, 14, 15]. Multi-Photon Ionization at 355 nm laser wavelength with a pulse width of 10 ns was used by Wang et al. [15] to detect acetone-water clusters with a TOF-MS. They found three series of acetone hydrated clusters isolated from the pure acetone, such as $(\text{CH}_3\text{COCH}_3)_m(\text{H}_2\text{O})_{m-2}\text{H}^+$, $(\text{CH}_3\text{COCH}_3)_m(\text{H}_2\text{O})_{m-1}\text{H}^+$ and $(\text{CH}_3\text{COCH}_3)_m(\text{H}_2\text{O})_m\text{H}^+$, and the domain series is $(\text{CH}_3\text{COCH}_3)_m(\text{H}_2\text{O})_{m-2}\text{H}^+$, while only one series of $(\text{CH}_3\text{COCH}_3)_m(\text{H}_2\text{O})_{m-2}\text{H}^+$ can be detected for clusters isolated from the acetone-water mixture with the volume ratio of acetone/water of 1:2. The clusters isolated from the 5% solution of acetone and liquid water were also detected by using a reflectron time of flight mass spectrometer and a femtosecond laser system by Hurley et al. [10], and protonated acetone clusters, acetyl-acetone clusters and acetone hydrated clusters species were evidently observed. The results of Wang et al. and Hurley et al. indicate that a microscopic phase separation occurs in acetone-water binary mixtures and depends on the volumetric ratio of acetone and water and on the ionization method.

In this work clusters of acetone-water binary mixtures in a wide range of acetone-water mixing ratios were detected by reflectron time of flight mass spectrometer using picosecond laser photo-ionization (PI) and electron ionization (EI), respectively, giving a further insight into the comprehension of the non-ideal mixing of acetone-water mixtures.

The lifetimes of both pure acetone and mixed acetone-water clusters are in the picoseconds time scale [10]

therefore a pico second pulse laser is appropriate to obtain their ionization with high efficiency, simultaneously reducing the fragmentation probability.

Experimental and Methods

The vapor samples were produced at a temperature of 28 °C, making a nitrogen gas flow bubbling in a reservoir filled with a solution (pure water or water–acetone mixture solution) at the entrance of the TOFMS. The TOFMS system was described in detail in a previous paper [17] and the experimental procedures employed in this work were already described in the previous paper of this series [8]. Briefly, the sampled gases enter the first chamber of the instrument through a solenoid actuated valve (Parker Hannifin Corporation, General Valve Division, Fairfield, NJ, USA) equipped with a 0.8 mm aperture nozzle generating a pulsed supersonic jet. The valve was modified in order to minimize the dead volume and to increase the suction efficiency. The central part of the jet is extracted by a skimmer to produce a pulsed molecular beam, which is ionized and analyzed by a Wiley-McLaren reflectron TOFMS instrument (Kaesdorf s.r.l., Munchen, Germany) where different types of ionization sources can be used.

The TOFMS system can be operated with a mass filter to deflect the lowest mass ions by a pulsed electric field so that the saturation of the detector (a microchannel plate-MCP) due to the very high signal intensities produced by the most abundant low-mass ions is avoided and the dynamic range of the detector is preserved. The use of the mass filter strongly reduces the signals below m/z 50, hindering the overloading of the detector by the most abundant and easily detectable low masses species. This is why afterwards the mass spectra will be reported starting from this m/z value.

For EI, the electrons are produced by a hot tungsten loop filament and accelerated to 70 eV kinetic energy. In the present experiments a pulse duration of 2 μ s with a repetition rate of 20 Hz was used for EI, in order to use the same frequency of the laser for a strict comparison between the two ionization methods.

A short pulse photo-ionization (PI) was also employed using the third harmonic of a Nd:YAG pulsed laser (Leopard Series model D-20; Continuum, Santa Clara, CA, USA) with a repetition rate of 20 Hz and pulse duration of 20 ps. The maximum peak energy was 7 mJ, while the corresponding Power Density (PD) was 2.81×10^{11} W/cm². A focusing lens was employed and the beam spot area was approximately 1.2×10^{-3} cm². Special grade (>99%) acetone was used, mixed with purified water with different volume and mole ratios. In this paper the acetone volumetric ratio V_A/V_S was defined as the ratio between the liquid acetone volume and the volume of solution and x_A as the corresponding molar ratio (ratio between acetone mole and total moles in water/acetone solution). The values of V_A/V_S and x_A employed are reported in Table 1.

Table 1. Acetone Volumetric Ratios V_A/V_S Studied in this Work and Corresponding Acetone Mole Fractions in the Liquid Solution x_A

V_A/V_S , %	x_A , mol/mol	V_A/V_S , %	x_A , mol/mol
0	0	10	0.0265
0.1	0.000245	15	0.0414
0.3	0.000736	20	0.0577
0.8	0.00197	25	0.0754
1.5	0.00371	30	0.0950
2.5	0.00624	35	0.116
5	0.0127	40	0.140

Results and Discussion

Mass Spectrometric Analysis of Acetone–Water Clusters

Mass spectra of clusters generated from acetone–water binary mixtures with different V_A/V_S ratios were measured by the TOFMS with EI and laser ionization. The mass spectra of clusters with EI and laser ionization were strongly dependent on the acetone–water mixing ratio.

Clusters mass spectra generated from acetone (A)–water (W) binary mixtures at $V_A/V_S = 0.3\%$ and 40% through the TOFMS system with EI are presented in Figures 1a1–b1. The clusters with the size up to m/z 700 were observed for the acetone–water binary mixture with different acetone solution ratio.

Figures 1a2–b2 report the cluster mass spectra with PI at the same acetone–water volumetric ratios. Clusters mass spectra at an intermediate concentration ($V_A/V_S = 5\%$) are reported in the Electronic Supplementary Material (Figure ESM. 1). It is clearly shown that the laser ionization increases the signal intensity and extends the mass range detection of the clusters in comparison with EI. The based peak intensities obtained with PI are 5–10 times higher when compared with EI, and, moreover, the highest peaks have also the increase of m/z 400–500 with the laser ionization at the same V_A/V_S . The spectral pattern changes markedly as V_A/V_S increases from 0.3% to 5%, and a slight change can be observed as V_A/V_S increases from 5% to 40%.

The comparison with a previous work [18] reveals that the clusters mass distribution is very similar to pure water clusters spectra only for the case of the more diluted solution ($V_A/V_S = 0.3\%$) (Figure 1a1 and a2), where the base peaks of the acetone–water clusters spectra are attributable to pure water clusters (peaks 73, 91 and 109, corresponding to $[(H_2O)_nH]^+$ with $n = 4, 5$ and 6). In all the other spectra, the base peaks are typical of mixed acetone–water clusters (peaks 101, 117, 193 and 269). These findings are in agreement with those obtained for ethanol–water clusters [8], except for the fact that at low volumetric ratios, ethanol–water clusters distributions, obtained with EI, were already characterized by mixed clusters, whereas the acetone–water clusters distributions obtained with EI are only characterized by pure water clusters. At $V_A/V_S > 5\%$ the mass spectra are dominated by neat acetone clusters $A_mW_nH^+$, with $n = 0$, and mixed A–W clusters $A_mW_nH^+$. The clusters families at fixed A and variable W are

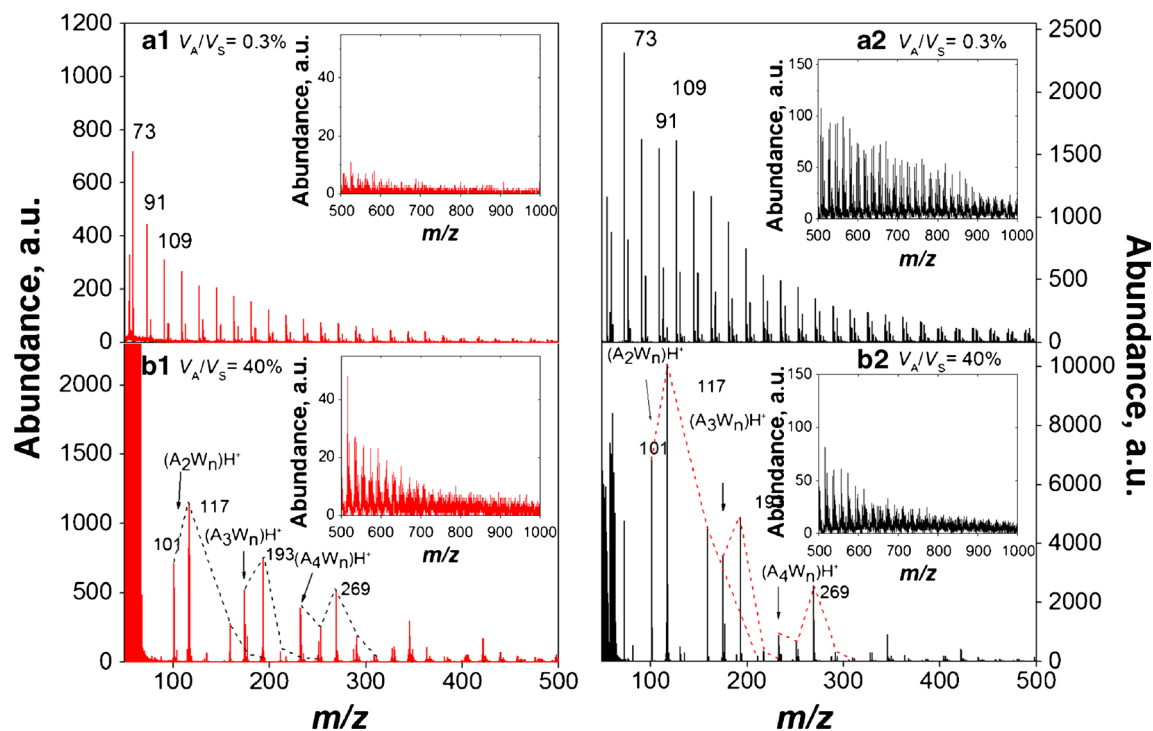


Figure 1. Mass spectra distribution of acetone–water clusters with different acetone/solution ratios with EI **(a1)** 0.3% V_A/V_S **(b1)** 40% V_A/V_S and with laser PI **(a2)** 0.3% V_A/V_S , **(b2)** 40% V_A/V_S . In b1–b2 $A_m W_n H^+$ are grouped. The series start from the $m = 2$ series with $n \geq 0$ (pure acetone clusters are present too)

grouped in the figures that show the main peak of each family attributable to neat acetone clusters, starting from the dimer. It can also be noticed that in the $A_m W_n H^+$ clusters families, at fixed m , monohydrated clusters show higher intensities than those with $n = 0$ and $n > 1$. In agreement with Shi et al. [19], it was also found the display of a magic number at $p = 21$ ($p = n + m$), as in the case of pure water clusters, which have enhanced abundance at the size $(H_2O)_{21}H^+$, corresponding to a clathrate structure where $(H_2O)_{20}$ forms a pentagonal dodecahedral cage with an H_3O^+ ion encaged [19, 20]. The intensity distributions of the mixed cluster size from $p = 19$ to $p = 24$, with the number of acetone molecules m in the cluster increasing from 3 to 5, are reported in the Electronic Supplementary Material (Fig. ESM. 2). In the figure a maximum at $p = 21$ is clearly observable. The same feature was found in the case of ethanol water clusters [8].

The changes into composition distribution of acetone–water clusters at different acetone volumetric ratios ($V_A/V_S = 0.3\%$ and 40%) with EI and PI are better observable in Figure 2. The distributions at an intermediate concentration ($V_A/V_S = 5\%$) are reported in the Electronic Supplementary Material (Figure ESM. 3).

In this figure the composition distribution of $(CH_3COCH_3)_m(H_2O)_nH^+$ (referred to in the following as $A_m W_n H^+$) clusters is sketched in a tridimensional graph, by reporting the abundance of detected cluster ions as a function of the number m (0–25) of acetone molecules and of the number n (0–55) of water molecules in each cluster.

The composition distributions of acetone–water clusters with EI are shown in Figure 2a1–b1. Owing to the great difference in the sensitivity at low masses and at high masses, cluster signals show rather steep intensity decreasing with increasing cluster size. It is clearly shown that the spectral pattern changed gradually and water-rich cluster signals became fainter, while acetone-rich cluster signals became higher with increasing acetone concentrations from 0.3% to 40%. At $V_A/V_S = 0.3\%$ (Figure 2a1), three similar mass distributions of water-rich series with $m = 0–2$ can be observed, and the main series can be seen as pure water clusters, $(H_2O)_nH^+$. This means that clusters distributions generated by acetone–water binary mixtures with very low acetone concentration show similar results to the ones obtained from pure water, as previously observed in studies on alcohol aqueous solutions and acetonitrile aqueous solutions [12, 13]. These findings indicate that hydrogen bonds between water molecules dominate the structure of the clusters in the solvent–water binary solution with a low solvent concentration. As V_A/V_S increases to 5% (see figure ESM. 3), some other series with $m = 5–10$ appear, while the maximum number of water in the clusters of each series significantly decreases. In this figure, it is shown that the main series are acetone hydrated clusters $A_m W_n H^+$ instead of pure water clusters, as it appears at $V_A/V_S = 0.3\%$. This suggests that the water hydrogen-bonding network in pure water has been removed from interaction with acetone already at $V_A/V_S = 5\%$, while, in the case of ethanol, this process occurred only at $V_E/V_S \geq 20\%$. In the

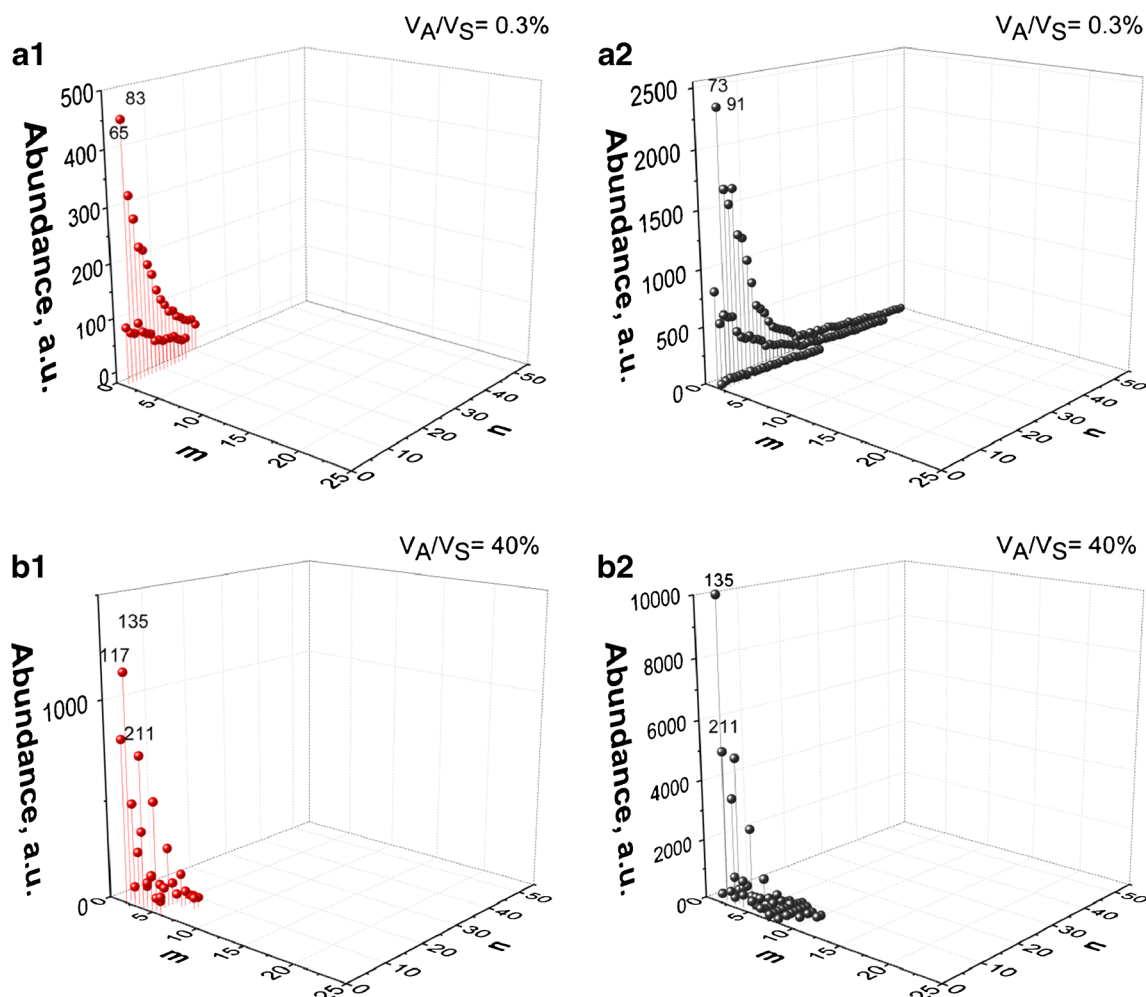


Figure 2. Composition distribution of acetone-water clusters, in terms of the number of water molecules (n) and acetone molecules (m) determined in each cluster, at different acetone/solution ratios with EI: **(a1)** 0.3% V_A/V_S , **(b1)** 40% V_A/V_S and with laser PI: **(a2)** 0.3% V_A/V_S , **(b2)** 40% V_A/V_S

acetone hydrated clusters series, the peaks following the trend $n = m - 2$, such as A_2H^+ , $A_3W_1H^+$, $A_4W_2H^+$ etc. can also be identified as at $V_A/V_S = 40\%$. The highest signals are attributable to clusters with $n < 4$ and $m < 8$, even though it is noteworthy to observe that big acetone clusters with m up to 10–15 are also formed. Due to the hydrogen bond acceptor character of acetone, its self-association is discouraged with respect to ethanol and the maximum number of acetone molecules in the clusters is 12, whereas it was 24 for ethanol.

This corresponds to the results obtained by Wang et al. and Hurley et al. [10, 15]. They suggest a role of water in mixed acetone-water clusters formation. Indeed, it was found, using the ab-initio calculations [15], that it is very easy for the acetone to form hydrogen bond clusters with water. And the protonated $(H_2O)_n H^+$ is the core of the clusters, which determines the structure of the clusters. Pure acetone clusters ($n = 0$) are also present but only up to 2 acetone molecules ($m = 2$) at $V_A/V_S = 0.3\%$ (Figure 2b1) and up to 8 acetone molecules ($m = 8$) at higher concentration [$V_A/V_S = 40\%$ (Figure 2b2)]. In literature pure acetone clusters up to $m = 4$ have been reported [21, 22].

A role of Van der Waals forces in self-association of acetone has to be claimed. In the literature [23], the interaction of the carbonyl groups with the methyl groups was hypothesized in the formation of pure acetone clusters. These weak interactions have been further confirmed by the use of hydrogen/deuterium substitution.

The fragments of acetone clusters, including $A_2CH_3^+$ and $A_2CH_3CO^+$, are also detected at $V_A/V_S = 5\%$ as shown in Figure ESM. 3. Hurley et al. also detected these fragments mass spectra with femtosecond laser ionization, while Wang et al. did not detect those with nanosecond laser ionization. The clusters structure has a correlation with the excess enthalpy of mixing. Acetone mixes with water exothermically in the low acetone mole mixing ratio ($x_A < 0.5$), according to Benedetti et al. [24]. This indicates that the interaction of acetone with water is energetically favorable and forms a stable cluster. As acetone was added to water, acetone-water interaction was promoted by the process of hydrogen-bonding. This corresponds to the results of infrared spectra of acetone mixture with water by Blair et al. [25], where a blue-shift occurs as acetone is

added to water with low acetone mole mixing ratio ($x_A < 0.3$). It indicates a strengthening in the structure or hydrogen bonding environment of liquid. The integration of the radial distribution functions (based on Monte Carlo simulations for hydrogen (water) – oxygen (acetone) site-site interaction) gives the co-ordination number increase from 0.17 to 1.27 with increasing water mole fractions from 0.125 to 0.875, which means that the average number of water molecules hydrogen bonded to a given acetone molecule increases as the water concentration raises [26]. It is shown that the series of pure water clusters completely disappear and the maximum number of water in the clusters of each series is less than 5 at $V_A/V_S = 40\%$. This is due to the ability of acetone to form relatively strong hydrogen bonds with water that would allow molecules to be dispersed more readily in acetone-rich mixture, and, as a consequence, there is a loss of high water connectivity according to Venables et al. [1].

The composition distributions of acetone-water clusters with laser ionization are shown in Figure 2a2–b2. Thanks to the high ionization efficiency of laser, more peaks corresponding to acetone-water clusters can be detected with laser ionization compared to EI. The variation of mass spectra distribution with the increase of V_A/V_S ratio shows the similar trend to that with EI, and this indicates that the microscopic phase separation for acetone-water binary mixtures is more markedly dependent on the V_A/V_S ratio than on ionization methods.

Autocorrelation Analysis of the Clusters Mass Spectra

The autocorrelation function (AF) was introduced to analyze the composition of the water clusters in terms of fundamental periodicities because the acetone-water clusters mass spectra are very complex and difficult to be interpreted. The application of AF on mass spectra analysis has been reported in details in previous papers [27, 28]. Briefly, AF can be defined as:

$$y(\tau) = \sum_0^{M-1} f(t)f(t-\tau)$$

Where $f(t)$ represents a signal of the length M , and $f(t-\tau)$ represents the delayed version of $f(t)$ by the time τ . The magnitude of the computed correlation shows the degree of similarity between the signals increasing the delay between two points. If the magnitude of the autocorrelation function is wide, the delayed signal will be considered to be very similar to the original one. Otherwise, if it is close to zero, the signal will be considered not keeping its linear relation increasing the distance between two points.

The transformed function has been evaluated as a function of m/z and reported as a function of the corresponding periodicity. The correlation of acetone-water clusters spectra at $V_A/V_S = 0.3\%$ and 40% with electron ionization from

m/z 50 to 500 is reported in Figure 3a1–b1. The results are normalized and the magnitude ranges from 0 to 1. The spectra at $V_A/V_S = 5\%$ are reported in the Electronic Supplementary Material (Figure ESM. 4). As shown in Figure 3a1, several significant correlations (normalized AF > 0.5), such as m/z 18, 36, 54, and 72 can be observed at $V_A/V_S = 0.3\%$. The notable peaks are at 18 units and its multiples at m/z 36, 54, 72, which represent water molecules. Increasing V_A/V_S ratio from 0.3% to 40%, the auto-correlation function for m/z 18 and its multiples decreases while it increases for the peaks of m/z 58 and 76, corresponding to the acetone molecule and $(\text{CH}_3\text{COCH}_3)(\text{H}_2\text{O})$ dimer (A_1W_1), respectively. Through the analysis of AF, it is easy to obtain the information of the composition of the clusters. And the significant correlation of m/z 18 and its multiples at $V_A/V_S = 0.3\%$ indicates that the mass spectrum is dominated by water-rich clusters, whereas the significant correlations of peaks m/z 58 and 76 at $V_A/V_S = 5\%$ and 40% indicate that the mass spectrum is dominated by acetone-rich clusters.

Similar results were observed for acetone-water clusters with PI (Figure 3a2–b2 and figure ESM. 4). The achievements were similar to those obtained with ethanol-water clusters and demonstrate the utility of AF for the analysis of complex and broad mass spectra.

Clusters Composition Distribution: Molar Ratio of Acetone to Water in the Observed Clusters (R_A)

The sum of peak intensities of cluster ions containing m molecules of acetone fragments is calculated as $\sum I_m$ (I : peak intensity). The sum ($\sum I_m$) multiplied by the number m , which is $m\sum I_m$, is assumed to be proportional to the total number of acetone fragment molecules in the cluster ions containing m molecules of acetone fragments. The sum ($\sum A$) of $m\sum I_m$ calculated from the whole mass spectrum is also assumed to be proportional to the total number of acetone fragment molecules in all cluster ions.

In the same way, indicating with I_n the peak intensity of cluster ions containing n molecules of water, the sum ($\sum W$) of $n\sum I_n$ calculated from the whole mass spectrum can be assumed to be proportional to the total number of water molecules in all ions. So, the intensity ratio of acetone to water, in the observed clusters, R_A value, can be calculated as: $\sum A/\sum W$.

Figure 4 reports the intensity ratio for acetone-water clusters with different ionization methods and concentrations. R_A for acetone-water with EI and laser ionizations increases with increasing acetone-solution volume ratio in all concentration range. In particular, a sharp increase occurs from $V_A/V_S = 0$ to 5–10% and, then, it increases gradually after $V_A/V_S = 5$ –10%. These findings are in agreement with the present mass spectrometric data as shown in Figure 1 (and ESM. 1), where the spectral pattern changes markedly as V_A/V_S increases from 0.3% to 5%, and only a slight change can be observed as V_A/V_S increases from 5% to 40%. Water-rich clusters signals

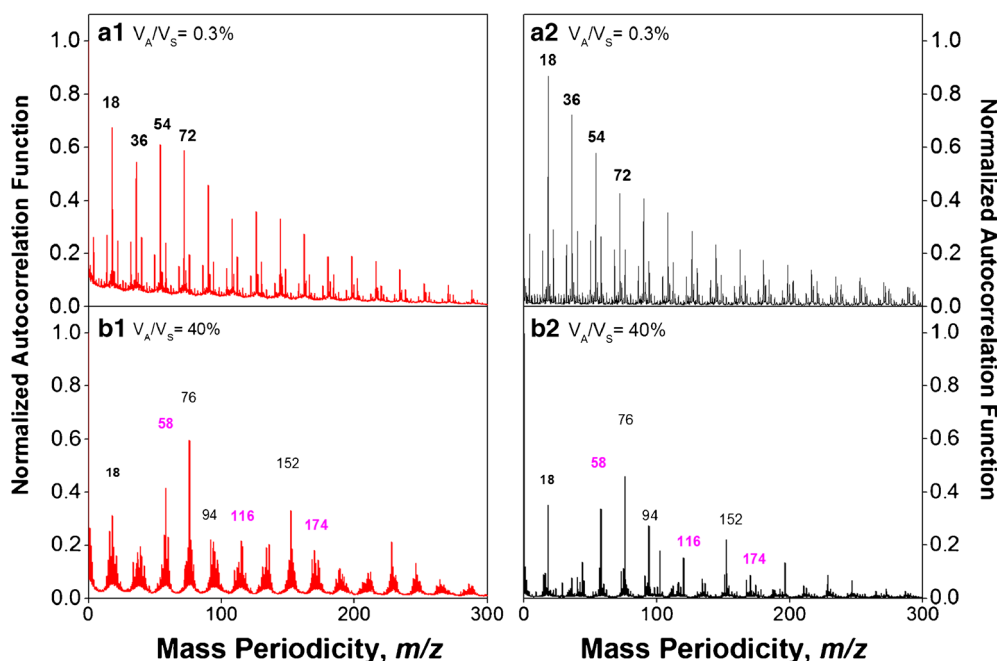


Figure 3. Autocorrelation of water clusters spectra with different acetone/solution ratios with EI: **(a1)** 0.3% V_A/V_S , **(b1)** 40% V_A/V_S and with laser PI: **(a2)** 0.3% V_A/V_S , **(b2)** 40% V_A/V_S . Labels for mixed acetone-water, pure water (*black, bolded*) and pure acetone (*magenta, bolded*) clusters are reported too

become fainter when increasing acetone concentrations over the whole composition range. The acetone concentration in the observed clusters is found to be much higher than that in the sample solution (acetone mole fraction x_A , also reported in the figure). This indicates that the microheterogeneity of the acetone-water binary mixtures should be composed of the acetone-rich clusters and the other water-rich part. In other words, acetone-water solutions show incomplete mixing at the molecular level.

It clearly shows that R_A strongly depends on the acetone concentration not on the ionization methods for lower acetone concentration solutions ($V_A/V_S < 5\text{--}10\%$) and that corresponds to the spectral pattern dominated by water-rich

clusters; while it inverses with a further rise in the acetone concentration. These achievements mean that R_A strongly depends on the ionization method instead of the acetone concentration for the solution at $V_A/V_S > 5\text{--}10\%$; and this is in conformity with the spectral pattern dominated by acetone-rich clusters. For example, R_A by laser ionization is 1.3 and 2 times higher than that by EI at $V_A/V_S = 10\%$ and 40%, respectively. This indicates that the ionization of water-rich clusters depends on the solution concentration, while the ionization of acetone-rich clusters depends on the ionization methods. This topic will be further discussed in part D.

Dependence of Cluster Mass Spectra on Laser Power Density (PD)

The mass spectra of clusters for the acetone-water binary mixtures at $V_A/V_S = 2\%$ and 20% with different laser power densities are shown in Figure 5. It is clearly shown that the signal intensities gradually decrease when the laser power density for both binary mixtures at $V_A/V_S = 2\%$ and 20% decreases.

The metastable fragment cluster ions (created in the field-free region of TOFMS as ionization energies are higher with respect to ionization threshold) can be easily discriminated in the reflectron section of the TOF mass spectrometer since they appear as satellites to the main unfragmented protonated cluster ion peaks [8, 29].

In Figure 6 $A_nW_nH^+$ parent and metastable fragment clusters distributions of acetone-water binary mixture solution at $V_A/V_S = 2\%$ obtained at different laser PD (in the range $1.20\text{--}2.81 \times 10^{11}$ W/cm², panels a1–e1) and with EI

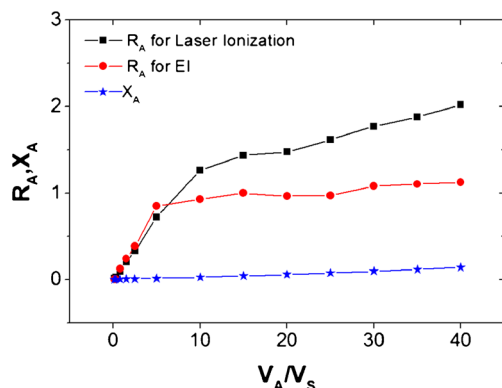


Figure 4. Comparison between the intensity ratio (R_A , see text for definition), obtained for EI and PI and acetone mole fractions in the liquid solution (x_A) at different V_A/V_S ratios. Errors are estimated to be about 10% for all R_A values and therefore not reported

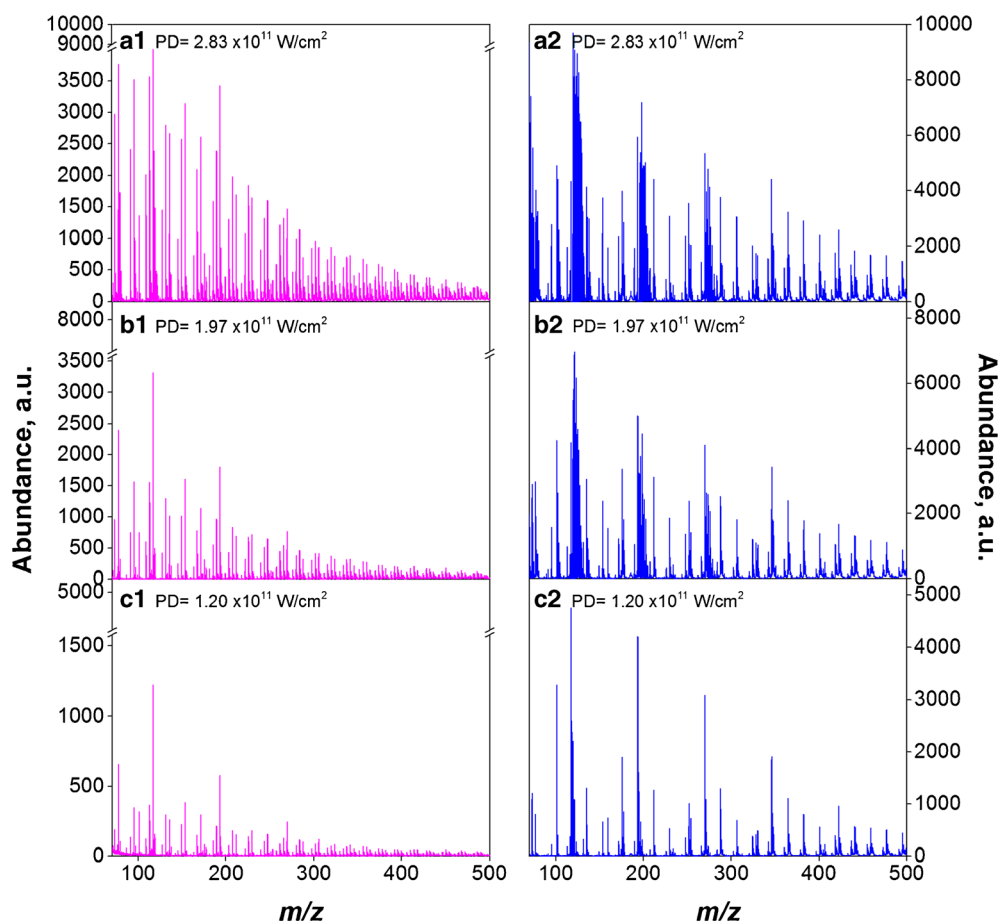


Figure 5. Mass spectra of clusters for the acetone–water solutions at $V_A/V_S = 2\%$ (series 1) and $V_A/V_S = 20\%$ (series 2) with PD 2.83 (a1, a2); 1.97 (b1, b2); 1.20 (c1, c2) $\times 10^{11}$ W/cm^2

(panel f1) are reported. The parent clusters intensities are much higher than those of metastable fragment clusters for small clusters ($n < 21$); while the signal intensity shows no significant difference between parent and metastable fragment for larger clusters ($n \geq 21$). The parent and metastable fragment clusters distributions with laser ionization are similar to those obtained using electron ionization as shown in Figure 6f1. These results are very similar to the studies on water clusters using photo-ionization [12] and chemical ionization [30]. This suggests that the formation of water-rich clusters and subsequent metastable fragmentation is the dominant process that causes the clusters distribution, apart from the initial ionization process. This also suggests that $A_l W_n H^+$ clusters distributions of the acetone water binary mixture solution with lower acetone concentration ($V_A/V_S = 2\%$) show similar characteristics with respect to the pure water clusters distribution.

Only the $A_{n+2} W_n H^+$ parent and metastable fragment clusters distributions of acetone-water binary mixture solution at $V_A/V_S = 20\%$, obtained at different PD and with EI, are presented in Figure 6 (series 2) since mass spectra for such mixture concentration are dominated by the clusters series $A_{n+2} W_n H^+$. It is clearly shown that the metastable fragment clusters peak is much higher than the ones of

parent clusters for small clusters ($n < 3$) in all the laser power densities other than 1.20×10^{11} W/cm^2 . This suggests that the ionization process significantly affects the acetone-rich clusters distribution, differently from what occurs with water-rich clusters.

The ratio of metastable fragmentation of the $A_l W_n H^+$ clusters at $V_A/V_S = 2\%$ is shown in the electronic supplementary material ESM. 5a1. The ratio of metastable fragmentation to the parent clusters intensity denoted as I_M/I_P , where I_M is the metastable fragment intensity and I_P is the parent clusters intensity. There are no significant differences between I_M/I_P in the laser power density range 1.20 – 2.82×10^{11} W/cm^2 . The ratio of metastable fragmentation of the $A_{n+2} W_n H^+$ clusters at $V_A/V_S = 20\%$ is reported in the electronic supplementary material (Fig. ESM. 5a2) and it is clearly shown that the values of I_M/I_P increase when increasing the laser power density. The higher value of I_M/I_P at higher laser power density suggests that more metastable fragmentation occurs in the drift region. This arises from photo-ionization threshold, which deposits more energy excess into the clusters. The different effect of the laser power density on the water-rich and acetone-water clusters might be related to the different ionization energies of acetone and water, which are 9.703 and 12.621 eV,

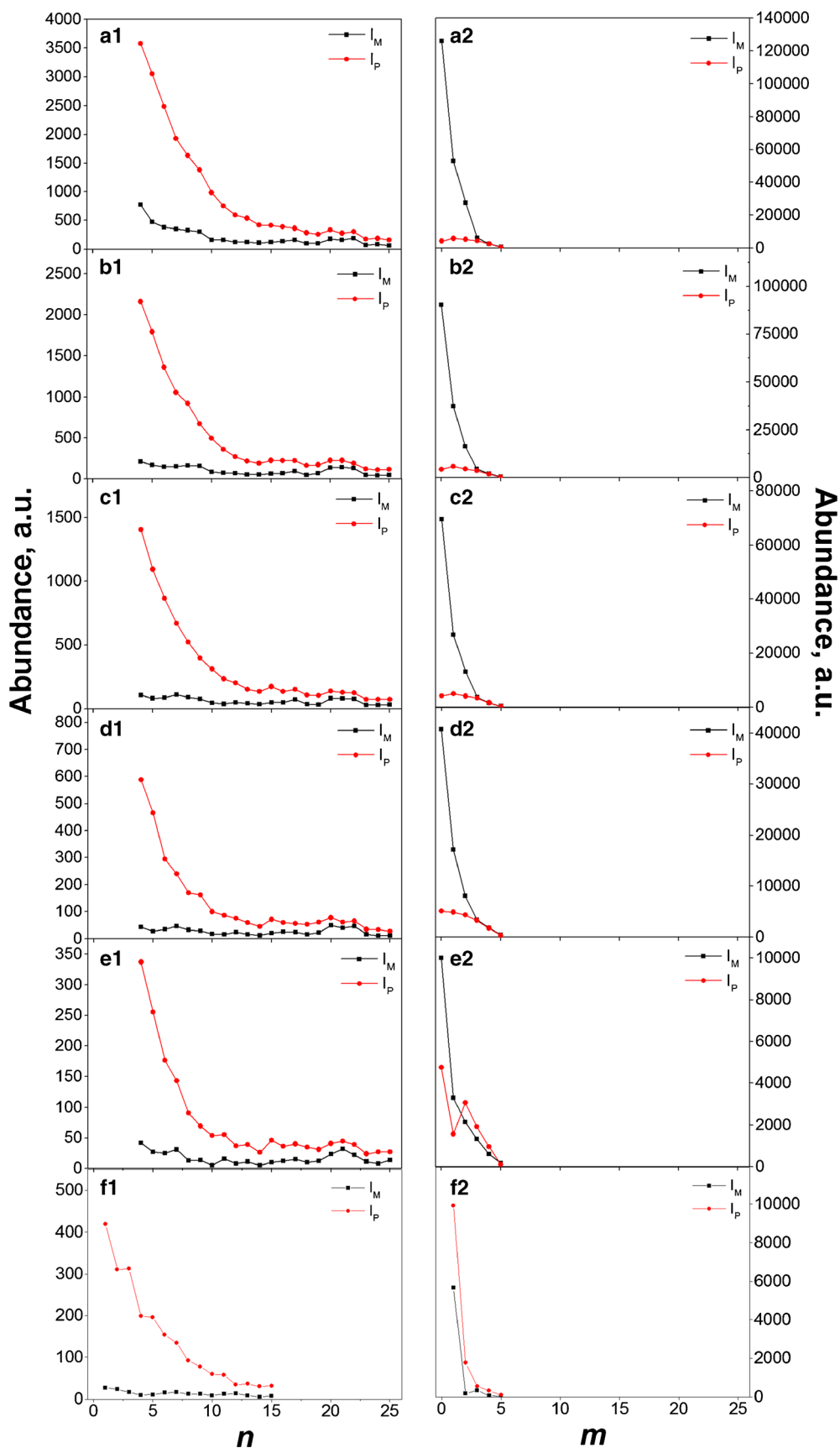


Figure 6. Metastable fragmentation of the the $A_7W_nH^+$ clusters at $V_A/V_S = 2\%$ (series 1) and A_mH^+ clusters at $V_A/V_S = 20\%$ (series 2) with PD 2.81 (a1, a2); 2.18 (b1, b2); 1.97 (c1, c2); 1.41 (d1, d2); 1.20 (e1, e2) $\times 10^{11}$ W/cm 2 $\times 10^{11}$ W/cm 2 and EI (f1, f2)

respectively. In the present experiments at 355 nm laser wavelength, the absorption of three photons would deposit a higher amount of energy (i.e. 10.5 eV) into the mixed clusters, thus promoting the metastable fragmentation to occur [31].

The occurrence of a three-photon ionization process has been demonstrated by reporting in bi-log plots the laser power density vs. signal intensity, shown in figure ESM. 6. The plots were obtained for series of water-rich clusters $A_nW_nH^+$ and acetone-rich clusters $A_{n+2}W_nH^+$, respectively. From the linear fit of bi-log plots it can be deduced that, for both water-rich clusters and acetone-rich clusters, nearly cubic laser energy dependence was observed, thus implying the occurrence of a three-photon ionization process.

Conclusions

In this paper, mass spectra of clusters generated by acetone-water binary mixtures with different V_A/V_S ratios were measured by the TOFMS with electron and laser ionization. The mass spectra of clusters with electron and laser ionization were strongly dependent on the acetone-water mixing ratio. The spectral pattern changed gradually and water-rich clusters signal became fainter whereas acetone-rich clusters signal became more intensive increasing acetone concentrations from 0.3% to 40%. Cluster distributions generated by acetone-water binary mixture with very low acetone concentration were found to be similar to those generated by pure water; while the water hydrogen-bonding network in pure water was changed by the interaction with acetone when acetone concentration increases.

The autocorrelation function (AF) was found to be an efficient method for the analysis of the variation of water clusters composition with the increase of the acetone concentration in terms of fundamental periodicities.

The intensity ratio for acetone-water clusters (R_A) strongly depended on the acetone concentration instead of ionization method for lower acetone concentration solution ($V_A/V_S < 5-10\%$). And that corresponded to the spectral pattern dominated by water-rich clusters, while it was inverted further increasing the acetone concentration. Indeed, R_A strongly depended on ionization method rather than on the acetone concentration for the solution at $V_A/V_S > 5-10\%$, which was corresponding to the spectral pattern dominated by acetone-rich clusters. This indicates that the ionization of water-rich clusters depends on the solution concentration, while the ionization of acetone-rich clusters depends on the ionization methods.

The formation of water-rich clusters and subsequent metastable fragmentation is the dominant process that determinates the clusters distribution, irrespective of the initial ionization process, while the initial ionization process significantly affects the acetone-rich clusters distribution.

Acknowledgments

The authors want to thank the MSE-CNR project 2013–2014 “Miglioramento dell’efficienza energetica dei sistemi di conversione locale di energia”, for the financial support.

References

- Mizuse, K., Kuo, J.-L., Fujii, A.: Structural trends of ionized water networks: infrared spectroscopy of water cluster radical cations $(H_2O)_n$ ($n = 3-11$). *Chem. Sci.* 2868–2876 (2011)
- Mizuse, K.: Spectroscopic investigations of hydrogen bond network structures in water clusters, pp. 1–12. Springer, Japan (2013)
- Venables, D.S., Schmuttenmaer, C.A.: Spectroscopy and dynamics of mixtures of water with acetone, acetonitrile and methanol. *J. Chem. Phys.* 113, 11222–11236 (2000)
- Matsumoto, M., Nishi, N., Furusawa, T., Saita, M., Takamuku, T., Yamagami, M., Yamaguchi, T.: Structure of clusters in ethanol–water binary solutions studied by mass spectrometry and X-Ray diffraction. *Bull. Chem. Soc. Jpn.* 68, 1775–1783 (1995)
- Nishi, N., Koga, K., Ohshima, C., Yamamoto, K., Nagashima, U., Nagami, K.: Molecular association in ethanol–water mixtures studied by mass spectrometric analysis of clusters generated through adiabatic expansion of liquid jets. *J. Am. Chem. Soc.* 110, 5246–5255 (1988)
- Nishi, N., Takahashi, S., Matsumoto, M., Tanaka, A., Muraya, K., Takamuku, T., Yamaguchi, T.: Hydrogen-bonded cluster formation and hydrophobic solute association in aqueous solutions of ethanol. *J. Phys. Chem.* 99, 462–468 (1995)
- Tsuchiya, M., Shida, Y., Kobayashi, K., Taniguchi, O., Okouchi, S.: Cluster composition distribution at the liquid surface of alcohol–water mixtures and evaporation processes studied by liquid ionization mass spectrometry. *Int. J. Mass. Spectrom.* 235, 229–241 (2004)
- Li, X., Wang, X., Passaro, M., Spinelli, N., Apicella, B.: Insights on clusters formation mechanism by time of flight mass spectrometry. 1. The case of ethanol–water clusters. *J. Am. Soc. Mass. Spectrom.* 26, 1665–1675 (2015)
- Bing, D., Hamashima, T., Fujii, A., Kuo, J.L.: Anticooperative effect induced by mixed solvation in $H+(CH_3OH)_m(H_2O)_n$ ($m+n=5$ and 6): a theoretical and infrared spectroscopic study. *J. Phys. Chem. A* 114, 8170–8177 (2010)
- Hurley, S.M., Dermota, T.E., Hydutsky, D.P., Castleman, J.: Ultrafast dynamics of acetone — Water clusters; the influence of solvation. *Int. J. Mass. Spectrom.* 228, 677–686 (2003)
- Wakisaka, A., Matsuura, K.: Microheterogeneity of ethanol–water binary mixtures observed at the cluster level. *J. Mol. Liq.* 129, 25–32 (2006)
- Wakisaka, A., Ohki, T.: Phase separation of water–alcohol binary mixtures induced by the microheterogeneity. *Faraday Discuss.* 129, 231–245 (2005)
- Wakisaka, A., Abdoul-Carime, H., Yamamoto, Y., Kiyozumi, Y.: Non-ideality of binary mixtures water–methanol and water–acetonitrile from the viewpoint of clustering structure. *Faraday Trans.* 94, 369–374 (1998)
- Raina, G., Kulkarni, U., Rao, C.N.R.: Mass spectrometric determination of the surface compositions of ethanol–water mixtures. *Int. J. Mass. Spectrom.* 212, 267–271 (2001)
- Wang, R., Kong, X.H., Zhang, S.D., Zhang, X., Fan, X.Y., Zhao, S.Y.: Multiphoton ionization of acetone–water clusters at 355 nm. *Opt. Lett.* 2, 396–398 (2006)
- Dixit, S., Crain, J., Poon, W.C.K., Finney, J.L., Soper, A.K.: Molecular segregation observed in a concentrated alcohol–water solution. *Nature* 416, 829–832 (2002)
- Panariello, M., Apicella, B., Armenante, M., Bruno, A., Ciajolo, A., Spinelli, N.: Analysis of polycyclic aromatic hydrocarbon sequences in a premixed laminar flame by On–line Time–Of–Flight Mass Spectrometry. *Rapid Commun. Mass Spectrom.* 22, 573–581 (2008)
- Apicella, B., Li, X., Passaro, M., Spinelli, N., Wang, X.: Multiphoton ionization of large water clusters. *J. Chem. Phys.* 140, 204313–204318 (2014)
- Shi, Z., Wei, S., Ford, J.V., Castleman, A.W.: Clathrate structures in water–methanol mixed clusters. *Chem. Phys. Lett.* 200, 142–146 (1992)
- Wei, S., Shi, Z., Castleman, A.W.: Mixed cluster ions as a structure probe: Experimental evidence for clathrate structure of $(H_2O)_{20}H^+$ and $(H_2O)_{27}H^+$. *J. Chem. Phys.* 94, 3268–3270 (1991)

21. Sharma, P., Vatsa, R.K.: Photochemistry of acetone clusters: size-dependent observation of Coulomb explosion in the multiphoton ionization regime. *EPL* **84**(43003), p1–p6 (2008)
22. Tzeng, W.B., Wei, S., Castleman Jr., A.W.: Multiphoton ionization of acetone clusters: metastable unimolecular decomposition of acetone cluster ions and the influence of solvation on intracuster ion-molecule reactions. *J. Am. Chem. Soc.* **111**, 6035–6040 (1989)
23. Guan, J., Hua, Y., Xie, M., Bernstein, E.R.: Weak carbonyl-methyl intermolecular interactions in acetone clusters explored by IR plus VUV spectroscopy. *Chem. Phys.* **405**, 117–123 (2012)
24. Benedetti, A.V., Cilense, M., Vollet, D.R., Montone, R.C.: Thermodynamic properties of liquid mixtures. III. Acetone—water. *Thermochim. Acta* **66**, 219–223 (1983)
25. Blair, J.T., Krogh-Jespersen, K., Levy, R.M.: Solvent effects on optical absorption spectra: the 1A₁–A₂ transition of formaldehyde in water. *J. Am. Chem. Soc.* **111**, 6948–6956 (1989)
26. Fretais, L.C.G., Cordeiro, J.M.M., Garbujo, F.L.L.: Theoretical studies of liquids by computer simulation: the water–acetone mixture. *J. Mol. Liq.* **79**, 1–15 (1999)
27. Bruno, A., Panariello, M., Apicella, B., Spinelli, N.: Proceedings of the 32nd meeting of the Italian section of Combustion Institute, Naples, Italy, April 26–28 (2009). <http://www.combustion-institute.it/proceedings/proc2009/data/I/I-12.pdf>
28. Apicella, B., Bruno, A., Wang, X., Spinelli, N.: Fast fourier transform and autocorrelation function for the analysis of complex mass spectra. *Int. J. Mass. Spectrom.* **338**, 30–38 (2013)
29. Ebata, T., Fujii, A., Mikami, N.: Vibrational spectroscopy of small-sized hydrogen-bonded clusters and their ions. *Int. Rev. Phys. Chem.* **17**, 331–361 (1998)
30. Kostko, O., Belau, L., Wilson, K.R., Ahmed, M.: Vacuum-ultraviolet (VUV) photoionization of small methanol and methanol–water clusters. *J. Phys. Chem. A* **112**, 9555–9562 (2008)
31. CRC Handbook of Chemistry and Physics, 78th edn. CRC Press, Boca Raton, FL, (1997)